Journal of Hydrology 663 (2025) 134218

Contents lists available at ScienceDirect

Journal of Hydrology

journal homepage: www.elsevier.com/locate/jhydrol

Research papers

# Herbaceous species richness enhances soil hydraulic conductivity by increasing soil pore connectivity

Huaqing Liu [a,b,c,f], Xiaodong Gao [a,b,c,e,f,*], Long Ma [d], Heng Liu [f], Xining Zhao [a,b,c,e,f]

[a] State Key Laboratory of Soil and Water Conservation and Desertification Control, Northwest A&F University, Yangling, Shaanxi 712100, China
[b] The Research Center of Soil and Water Conservation and Ecological Environment, Chinese Academy of Sciences and Ministry of Education, Yangling, Shaanxi 712100, China
[c] Institute of Soil and Water Conservation, Chinese Academy of Sciences and Ministry of Water Resources, Yangling 712100, China
[d] College of Water Resources and Architectural Engineering, Northwest A & F University, Yangling, Shaanxi 712100, China
[e] College of Soil and Water Conservation Science and Engineering, Northwest A & F University, Yangling, Shaanxi 712100, China
[f] University of Chinese Academy of Sciences, Beijing 100049, China

ARTICLE INFO

This manuscript was handled by Dr marco borga, Editor-in-Chief, with the assistance of Hanbo Yang, Ph.D., Associate Editor

*Keywords:*
Plant diversity
CT
Soil structure
Biopores
Fractal dimension

ABSTRACT

Soil pore characteristics play a crucial role in determining soil hydrological processes. Plant diversity is recognized as a key factor in regulating soil hydraulic conductivity. However, the mechanisms by which plant diversity influencing soil pore characteristics and, consequently, hydraulic conductivity remain unclear. This study investigated the effects of herbaceous plant species richness on soil pore structure and its influence on both saturated and near-saturated hydraulic conductivity. A controlled experiment was conducted with four levels of herbaceous plant species richness (monoculture to four-species mixtures), coupled with soil pore analysis using X-ray computed tomography and measurements of saturated and near-saturated hydraulic conductivity. Our results showed that increasing plant diversity significantly increased soil porosity, particularly at plant richness levels of three and four species. This increase was primarily driven by an increase in connected porosity and a decrease in isolated porosity. Furthermore, the fractal dimension of both total pores and connected pores increased with increasing species richness. We found significant positive correlations between both near-saturated and saturated hydraulic conductivity and several pore characteristics including total porosity, connected porosity, connected pores, the fractal dimension, total biopores volume, and the specific characteristic of biopores. In-depth analysis indicated that saturated hydraulic conductivity was positively influenced by species richness, both directly through increased connected porosity and indirectly through changes in biopore volume, shape factor, and equivalent diameter. Additionally, species richness enhanced near-saturated hydraulic conductivity by increasing connected porosity and the shape factor of biopores. Our findings highlight the importance of plant diversity in regulating soil pore structure and enhancing hydraulic conductivity, contributing to a better understanding of the coupled plant-soil-hydrology processes and suggesting implications for sustainable ecosystem management.

## 1. Introduction

Plant diversity can enhance plant productivity and promote nutrient accumulation, making it a critical component for achieving Sustainable Development Goals (SDGs), particularly SDG 6 (Clean Water and Sanitation), SDG 13 (Climate Action), and SDG 15 (Life on Land) (Blicharska et al., 2019; Isbell et al., 2011; Lange et al., 2019; Tilman, 2000). Plant diversity plays a crucial role in regulating water cycle processes, including evapotranspiration, surface runoff, and soil infiltration (Fischer et al., 2015; Liu et al., 2025; Ma et al., 2024b). Recent experimental evidence demonstrates that multi-species cover crop systems can significantly enhance soil hydraulic functions. For example, Haruna et al. (2023) reported that a two-year mixed cover crop rotation (wheat-clover-triticale-vetch) reduced bulk density by 17 % and

* Corresponding author at: State Key Laboratory of Soil and Water Conservation and Desertification Control, Northwest A&F University, Yangling, Shaanxi 712100, China.

*E-mail address:* gao_xiaodong@nwafu.edu.cn (X. Gao).

https://doi.org/10.1016/j.jhydrol.2025.134218
Received 1 June 2025; Received in revised form 18 August 2025; Accepted 4 September 2025
Available online 7 September 2025

increased macroporosity-driven saturated hydraulic conductivity ($K_{sat}$) by 23–28 % compared to monoculture systems, though they cautioned about temporal variability in these effects. Soil hydraulic conductivity (the ability of soil to transmit water under unit hydraulic gradient) is a fundamental property that governs key hydrological processes such as infiltration (the process of water entry at the soil surface), while preferential flow (channelized movement through macropores) operates largely independent of matrix hydraulic conductivity and is instead controlled by macropore characteristics and connectivity (Blanchy et al., 2023; Hillel, 2003). Understanding how plant diversity influences soil hydraulic conductivity is essential for sustainable water resource management and mitigating the impacts of climate change.

Plant diversity affects soil hydraulic conductivity through various mechanisms that may regulate soil pore characteristics. Soil pore characteristics, including volume, size, shape, and connectivity, play a crucial role in determining the retention and transport of water (Houston et al., 2017; Koestel et al., 2018; Schlüter et al., 2020; Zheng et al., 2022). Underlying these characteristics is the soil pore system, which refers to the interconnected network of pores of varying sizes and shapes within the soil matrix (Wang and Zhang, 2024). The specific arrangement and attributes of this network, known as pore structure, describe the geometric arrangement and characteristics of these pores (Rabot et al., 2018). The formation of soil pores is mainly affected by plant growth (Lucas et al., 2022), soil fauna activities (Stolze et al., 2022) and management practices (Ferreira et al., 2023). For example, Bodner et al. (2023) demonstrated that transitioning from conventional to soil-health-oriented farming systems can partially restore soil pore characteristics by promoting biological agents of structure formation and increasing the soil organic carbon to clay ratio. Previous studies have reported that plant diversity affects plant growth and soil fauna activity (Korboulewsky et al., 2016; Zhang et al., 2022b), which in turn may influence soil porosity and pore characteristics, ultimately affecting soil hydraulic conductivity.

Diverse plant communities exhibit a wide range of root architectures, resulting in variations in root depth, density, and branching patterns (Oram, 2018; Yang et al., 2022). This diverse root system architecture can create complex networks of biopores that enhance soil aeration, drainage, and water infiltration (Nespoulous et al., 2019; Zhang et al., 2024). For example, species with deep taproots can create macropores that facilitate rapid infiltration, while species with dense, fibrous root systems can enhance the connectivity of smaller pores (Shao et al., 2024; Tang et al., 2024). Wu et al. (2016) found that grass mixtures improve soil infiltration rate due to their greater root biomasses. In grasslands sown with multiple species, root channels increased soil infiltration capacity (Wu et al., 2017). Besides live roots, decayed roots may also play a significant role in increasing the soil water-holding capacity (Cui et al., 2022). Furthermore, plant diversity can increase soil organic matter content and composition, leading to improved soil aggregation and enhanced water infiltration (Bucka et al., 2019; Gould et al., 2016; Liu et al., 2024; Ma et al., 2023). Ma et al. (2024a) found that the effect of mixed roots on saturated conductivity was mainly achieved by indirectly affecting soil organic matter. These factors collectively influence the relationship between plant diversity and soil hydraulic conductivity. However, the literature also reports instances of no or negative effects of plant diversity on soil hydraulic parameters (Gould et al., 2016; Ni et al., 2018), potentially due to factors such as specific plant species combinations, competition for resources, or environmental conditions. Unlike root characteristics, soil organic matter, and soil structure indicators, soil pore characteristics directly determine water retention and movement within the soil.

Advances in X-ray computed tomography (XCT) have facilitated the acquisition of 3D data on soil pore systems, providing more detailed information about soil pore characteristics than traditional methods like bulk density measurement and soil moisture characteristic curves (Talukder et al., 2023; Zhang et al., 2023). While bulk density measurements can estimate total porosity, they do not capture the complexity of pore morphology, which is crucial for understanding water movement in soil. Different pore characteristics, as described by morphology parameters (with their descriptions and calculation methods detailed in Table 1), exhibit varying relationships and contributions to soil hydraulic conductivity under different conditions. Soil hydraulic properties are strongly influenced by the structure and connectivity of soil pores, which can be affected by various biotic and abiotic factors, such as root growth, soil compaction, and tillage practices (Qian et al., 2024). Within the complex soil matrix, the relationship between pore characteristics and hydraulic conductivity is not always consistent; while many studies link hydraulic conductivity to pore connectivity (Casali et al., 2024; Chen et al., 2022; Vervoort and Cattle, 2003), others have found no such relationship, particularly regarding preferential flow (Fukumasu et al., 2024). While previous studies have investigated the effects of plant diversity on bulk soil properties (Fischer et al., 2015), our understanding of how plant diversity influences the detailed three-dimensional structure of soil pores remains limited. Nondestructive techniques like XCT scanning can more accurately characterize soil pore morphology, helping to elucidate the regulatory role of these pores in the relationship between plant diversity and soil hydraulic properties.

Therefore, the present study aims to elucidate how herbaceous plant diversity modifies soil pore structure and, in turn, influences both saturated and near-saturated hydraulic conductivity. We hypothesize that increasing herbaceous plant diversity, through the development of diverse root systems and increased biopore formation, will alter soil pore characteristics and specifically enhance macropore connectivity and create more tortuous flow pathways, leading to higher saturated and near-saturated hydraulic conductivity. The findings of this study will contribute to a better understanding of the coupled plant-soil-hydrology processes and provide scientific evidence for the management of plant diversity to improve ecosystem hydrological functions.

## 2. Materials and methods

### 2.1. Study sites

The experiment was conducted at the Soil and Water Conservation Field Science Experiment Station (108°07′E, 34°20′N) in Yangling District, Shaanxi Province, China. The site exhibits a continental monsoon climate, with an average annual temperature of 13 °C. Extreme temperatures range from 42 °C in summer to –19.4 °C in winter, with an average annual precipitation of 610.2 mm and evaporation of 1505.3 mm. The soil in the experimental area is composed of 28.73 % sand, 40.12 % silt, and 31.15 % clay, with a bulk density of 1.28 g $cm^{-3}$.

### 2.2. Experiment design

In March 2022, 36 experimental plots (2×1 m) were established, each equipped with two tubes for measuring soil moisture using a portable time domain reflectometer sensor (Trime-pico IPH/T3) during sampling (Liu et al., 2024). The experiment involved four common forage species: *Medicago sativa* (M), *Astragalus adsurgens* (A), *Elymus dahuricus* (E), and *Bromus inermis* (B), which were planted in different combinations: single species (M, A, E, B, denoted as T1), two species (M+E, M+B, A+E, A+B, T2), three species (B+A +E, B+M+E, T3), and four species (M+A+E+B, T4), as well as a control treatment (CK) with no planting. The selection of species was based on the following criteria: 1) priority was given to native plants with strong adaptability and excellent ecological restoration functions; (2) species were reasonably matched based on morphological, phenological, and physiological characteristics to promote complementary advantages; (3) seed availability and suitability for large-scale cultivation were also considered. Each treatment had three replicate plots, resulting in a total of 36 plots. The target planting densities were as follows: M: 1.5 g $m^{-2}$, A: 1.5 g $m^{-2}$, E: 3 g $m^{-2}$, and B: 3 g $m^{-2}$. The seeding densities were referenced from

**Table 1**
Descriptions of the pore characteristics.

| Pore characteristics | Description and calculate method | Function related to soil hydraulic |
|---|---|---|
| Porosity | The percentage of total pore space volume relative to the total volume of the region of interest (Larsbo et al., 2014). | Total porosity positive correlated with $K_{sat}$ (An et al., 2022; Vervoort and Cattle, 2003). |
| Connected porosity | Percentage of pore space that is interconnected and allows fluid flow (Larsbo et al., 2014). | Connected porosity, which has the greatest impact on permeability (Ling et al., 2022), has been positively correlated with both $K_{sat}$ (An et al., 2022) and $K_{usat}$ (Müller et al., 2018). |
| Isolated porosity | Percentage of pore space that is isolated and does not contribute to fluid flow (Larsbo et al., 2014). | |
| Global connectivity | The ratio of the connected porosity and the total porosity (Naveed et al., 2016). | Pore connectivity, especially global connectivity, contributes to increased hydraulic conductivity (Klöffel et al., 2024) and is crucial for estimating $K_{sat}$ and near-saturated hydraulic conductivity ($K_{nsat}$, Larsbo et al., 2014; Zhang et al., 2019). |
| Critical pore diameter (dc) | The largest sphere that can pass through the pore system form top to bottom (Jarvis et al., 2017). | The critical pore diameter has been shown to be a strong predictor of permeability (Qian et al., 2024) and is positively correlated with $K_{sat}$ (Klöffel et al., 2024; Koestel and Schlüter, 2019). |
| Length | Maximum of the ferret diameters (Fang et al., 2024). | Pore size affects water flow in soil (Yu et al., 2019). |
| Width | Minimum of the ferret diameters (Fang et al., 2024). | Pore size affects water flow in soil (Yu et al., 2019). |
| EqDiameter (EqD) | Equivalent diameter represents the diameter of the shape of the same volume (Herlinger and Vidal, 2022). | EqDiameter based pore size significantly affect permeability (Luo et al., 2024). |
| Thickness | Thickness of pores in 3D space. Reflects pore geometry (Luo et al., 2010). | Pore size affects water flow in soil (Yu et al., 2019). |
| Area | Area of the object boundary (Herlinger and Vidal, 2022). | The results of permeability simulations showed the permeability increased with the increase of 2D/3D pores size (Yu et al., 2019). |
| Volume | The number of voxels of the object multiplied by the volume of a single voxel. | |
| Fractal dimension (FD) | Measure of the complexity and self-similarity of the pore network (Rieu and Sposito, 1991). FD increases with the complex of structure (Wang et al., 2019). | Fractal dimension is significantly positively correlated with both $K_{sat}$ (Ju et al., 2024) and solute preferential transport (Fukumasu et al., 2024; Luo et al., 2024). |
| Shape_VA3d (Shape) | Shape_VA3d is shape factor described as sphericity$^{-3}$ (Herlinger and Vidal, 2022). The value of Shape_VA3d is computed using the formula $A^3/(36\pi V^2)$, a value of 1 corresponds to a perfect sphere. In contrast, larger values suggest less compact objects. | The air–water flow rate decreases as the shape factor decreases(Chen et al., 2022). |
| Hydraulic radius (HR) | The hydraulic radius is calculated as the ratio of the pore volume to the pore surface area (HR = Pore Volume / Pore Surface Area) (Larsbo et al., 2014). | Hydraulic radius positive with permeability (Ju et al., 2024; Larsbo et al., 2014; Qian et al., 2024). |
| Multifractal parameter (Δα) | Quantify spatial heterogeneity via singularity spectrum width. | Singularity spectrum width negative with $K_{sat}$ (Ju et al., 2021). |

the densities widely used for these species in local agricultural practices. To achieve these densities, seeds of each species were weighed and carefully distributed within each plot to ensure even spacing. Each treatment had three replicates. Seeds were sown at the end of April 2022. No fertilization or irrigation was applied during the experiment. Weeds were manually removed as needed to maintain the desired species composition in each plot.

### 2.3. Soil sampling and laboratory analysis

Soil samples were collected in April 2024. Soil samples for physicochemical analyses were collected form 0–20 cm depth using a soil auger with a 5 cm diameter. These samples were sieved to 2 mm and air-dried prior to physicochemical analyses. For saturated hydraulic conductivity measurements, one undisturbed soil cores were collected from each plot at a depth of 5–10 cm using cutting rings (100 cm$^3$). The soil cores were carefully extracted to minimize disturbance and were transported to the laboratory in sealed plastic bags to maintain their moisture content. For XCT scanning, undisturbed soil cores (5 cm diameter and 7 cm height) were collected using PVC pipes. The cores were carefully trimmed to fit the sample holder of the XCT scanner, ensuring minimal disturbance to the soil structure. One soil core was collected from the center of each plot at a depth of 3–10 cm. As each species and species combination treatment had three replicate plots, this resulted in 3, 12, 12, 6, and 3 measurement points for CK, T1, T2, T3, and T4 treatments, respectively.

Soil organic carbon was determined using the dichromate oxidation–reduction colorimetric method. Total nitrogen content (TN) was measured using the Kjeldahl method. Soil ammonium nitrogen ($NH_4^+$-N) and nitrate nitrogen ($NO_3^-$-N) were analyzed using a flow analyzer. Dissolved organic carbon (DOC) was extracted with distilled water in a 5:1 soil: water ratio and measured using a Shimadzu TOC analyzer (TOC-V, Shimadzu, Japan) (Zhang et al., 2022a).

### 2.4. X-ray CT measurement, image processing and analysis

The undisturbed soil columns were scanned using a Nano Voxel 1280 industrial CT imaging scanner (Tianjin Sanying Precision Instruments Co., Ltd., China). The peak voltage was set to 80 kV, and the maximum resolution was 40 μm with an exposure time of 0.2 s. The samples were fixed on the sample stage and rotated 360° horizontally, with a total of 1,280 projection images collected for each soil column with resolution of 47.4356 μm. The CT software was used to eliminate ring artifacts and reconstruct the images.

After the XCT tests, raw images were processed using a combination of VoxelStudioRecon, Avizo and Fiji software. First, raw CT scan data were reconstructed using VoxelStudioRecon software, and ring artifacts were removed during this step. After reconstruction, images were imported into Avizo software where the following sequential steps were applied: (1) Crop Editor [cropping to 800$^3$ voxel cubes]; (2) Filter [a) Non-Local Means Filtering (spatial standard deviation of 1, intensity standard deviation of 0.3, search window of 10 voxels, and local neighborhood of 5 voxels); b) Ring Artifact Removal (radius of 400); c) Unsharp masking (radius of 4 voxels, edge contrast of 0.7, and brightness threshold of 0)] (Ferreira et al., 2022); (3) Interactive Thresholding [threshold was based on the peak values in the image's gray value distribution histogram]; (4) Interactive Top-Hat [Black Top hat type and 3D Connectivity of 26]; (5) And Image [combined both segmentation images]; (6) Label Analysis [Porosity, morphological features (as listed in Table 1), and connectivity of the segmented pores were calculated using Avizo software]; (7) 3D Gray Multifractal analysis Boxing counting [the segmented pore images were processed using the Multifractal plugin in Fiji software to calculate multifractal parameter; (8) ExtractBiopores [the segmented pore images were processed using the SoilJ plugin in Fiji software to calculate critical pore diameter and identify biopores (Koestel, 2018)]; (9) Label Analysis [Porosity and morphological features of the biopores were calculated]. The test and analysis flow are shown in Fig. 1.

### 2.5. Soil saturated and near-saturated hydraulic conductivity

Soil saturated hydraulic conductivity was measured constant water head method described by Wang et al. (2018). Rings collected from filed were slowly saturated over a 48 h period, then put it into a permeameter and recorded water volume drop form cutting ring per 30 min until it stable. $K_{sat}$ values were calculated using Eq (1).

$$K_{sat} = \frac{10 \times Q_n \times L}{\tan \times S \times (h + L)} \tag{1}$$

where, $K_{sat}$ is the soil saturated hydraulic conductivity (cm min$^{-1}$); $Q_n$ is stable water volume (cm$^{-3}$); tan is the interval of water samples (min); $S$ is the cross-sectional area of ring; $h$ is water head (cm); $L$ is soil layer (cm).

Near-saturated hydraulic conductivity was determined using a tension infiltrometer (Meter Group® Mini Disk infiltrometer) under the tension of 0.02 m (Webb et al., 2022), which is commonly used in field measurement (Quigley et al., 2021; Zhao et al., 2014). Field measurements followed the same experimental design and replication scheme as the soil sampling detailed in Section 2.3. One measurement point was selected in the center of each plot. At each point, we recorded water level every minute until the values stable.

Near-saturated hydraulic conductivity was calculated based on the cumulative infiltration data using Zhang (1997)'s theoretical framework (Eqs. 2–4). The van Genuchten-Mualem model, fitted via Levenberg-Marquardt algorithm in an Excel macro (Ramos et al., 2006), represents the standard analytical for tension disk infiltrometer data processing. Although root-induced pore rearrangement may challenge the assumption of spatially random pore distribution(Wang et al., 2025), we prioritized this established methodology because Mualem's model is a well-established and widely adopted method for estimating hydraulic conductivity in both bare and rooted soils (Gregory et al., 2010; Rujner et al., 2018). Its use in numerous studies facilitates direct comparison with existing literature.

$$I = C_1 t^{1/2} + C_2 t \tag{2}$$

where, $I$ is the cumulative infiltration rate (cm); $t$ is time (min); $C_1$ is the correlation coefficient of soil hydraulic conductivity (cm min$^{-0.5}$); $C_2$ is the soil water sorptivity coefficient (cm min$^{-1}$).

$$K_{nsat} = \frac{C_2}{A} \tag{3}$$

$$A = \frac{11.65\,(n^{0.1} - 1)\exp^{(7.50(n-1.9)\,\alpha h_0)}, n < 1.9}{(\alpha r)^{0.91}} \tag{4}$$

where, $K_{nsat}$ is near-saturated hydraulic conductivity (cm min$^{-1}$), which can be converted to mm min$^{-1}$ by multiplying the value by 10; $A$ is a dimensionless coefficient; $r$ is the radius of the disk (cm); $n$ and α are the van Genuchten moisture retention parameters; and $h_0$ is the applied pressure head at the disk (cm). We use values of 1.31 and 0.019 cm$^{-1}$, respectively, for $N$ and $\alpha$, as these parameters were obtained from the instrument manual based on the soil types.

### 2.6. Statistical analysis

To account for the nested structure of our experimental design (species combinations nested within species richness levels), we used mixed-effects models for analyzing the data. We performed analysis of

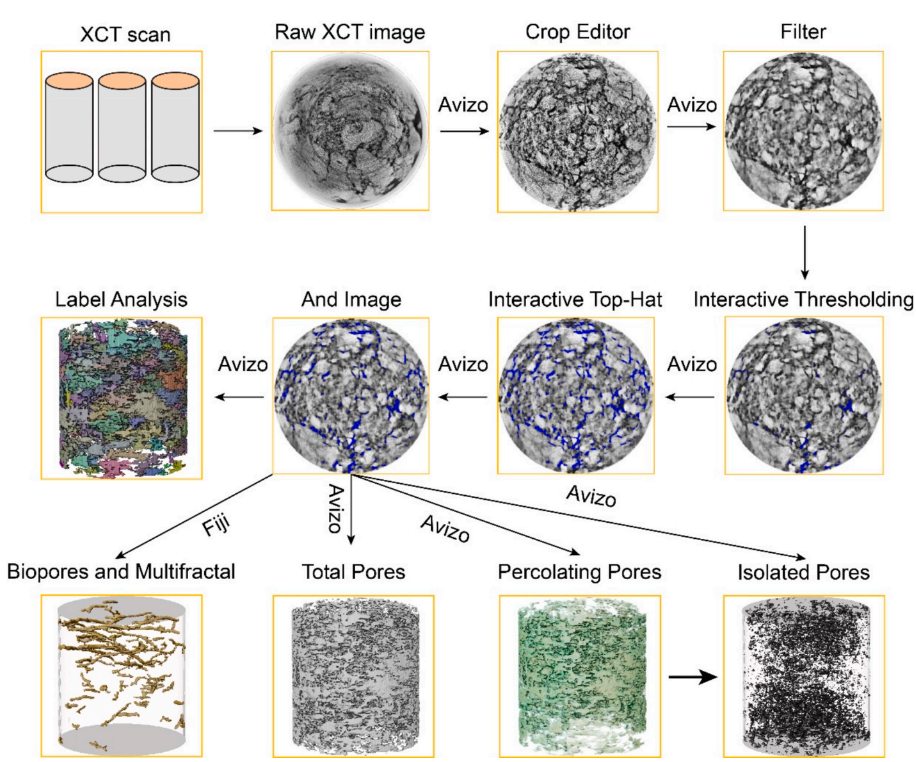


**Fig. 1.** Flowchart of XCT data processing and analysis.

variance (ANOVA) using the aov(Y ~ SR/Species, data) function in R, where Y represents the analyzed variable (e.g., porosity, morphological parameters), SR represents species richness levels, and Species represents the specific species combinations nested within each richness level. Additionally, non-parametric Kruskal–Wallis test was used to evaluate the effect of species richness on soil pore properties, hydraulic conductivity and soil organic physicochemical properties. Correlations between species richness and soil pore properties and hydraulic conductivity were also evaluated using pearson correlation.

Piecewise structure modeling was used to analyze the effect of species on soil pore properties and hydraulic conductivity (Lefcheck, 2016). For structural equation modeling, we used the *'nlme'* package in R to construct a mixed-effects model with the same nested structure as described above (José et al., 2024). This approach allowed us to account for the potential dependence of observations within each species richness level.

All analyses were performed in R version 4.3.1 (R Development Core Team, 2023), Other R packages used for data analysis and visualization included *'ggplot2'* (Wickham et al., 2024), *'ggpubr'* (Kassambara, 2023), and *'Hmisc'* (Frank and Charles, 2024).

## 3. Results

### 3.1. Soil porosity characteristics measured by X-ray CT

The effects of species richness on soil porosity, fractal dimension, and other properties are shown in Fig. 2 and Table 2. After the herbaceous plants were planted, regardless of the number of species, soil total porosity and connected porosity increased, while isolated porosity decreased. Additionally, the fractal dimensions of both total pores and connected pores increased. The bare soil treatment had a total porosity of 10.36 %, with fractal dimensions of 2.39. For varying levels of species richness, total porosity and connected porosity increased with increasing species number. Among the treatments, the highest values for total porosity and connected porosity were observed with three species, reaching 19.20 % and 18.55 %, respectively, representing increases of 85.33 % compared to the single-species treatment. The lowest isolated porosity was also observed with four species, at 0.63 %, a decrease of 47.37 % compared to monoculture treatment. The fractal dimensions of both total pores and connected pores in different species richness treatments showed a slight increasing trend.

The vertical distribution of soil porosity within the soil columns is presented in Fig. 3A. For all treatments, total porosity and connected porosity exhibited similar patterns. After the establishment of herbaceous plant communities, total porosity and connected porosity in the 0–4 cm depth, with the increase becoming more pronounced with increasing species richness. Conversely, isolated porosity showed an opposite trend. Figs. 3B, 3D, and 3F illustrate the distribution of porosity across different equivalent diameters, lengths, and widths of connected

**Table 2**
Soil characters under different treatments. The data are presented as mean values with standard deviations in parentheses. The treatments include monocultures (T1), two-species mixtures (T2), three-species mixtures (T3), four-species mixtures (T4), and no planted bare land (CK).

| Variable | T1 | T2 | T3 | T4 | CK |
|---|---|---|---|---|---|
| SOC (g kg$^{-1}$) | 4.38 (0.60) | 4.03 (0.65) | 4.46 (0.69) | 4.80 (0.76) | 4.70 (0.71) |
| TN (g kg$^{-1}$) | 0.50 (0.05) | 0.48 (0.04) | 0.52 (0.06) | 0.53 (0.07) | 0.48 (0.05) |
| CNR | 8.95 (1.34) | 8.39 (0.93) | 8.66 (1.14) | 9.09 (0.46) | 9.76 (0.79) |
| DOC (mg kg$^{-1}$) | 7.52 (3.34) | 5.38 (3.83) | 4.94 (2.36) | 5.80 (1.77) | 6.12 (3.05) |
| $NH_4$–N (mg kg$^{-1}$) | 1.09 (0.47) | 1.08 (0.53) | 1.17 (0.67) | 1.56 (0.63) | 0.99 (1.06) |
| $NN_3$–N (mg kg$^{-1}$) | 1.45 (1.04) | 0.91 (0.76) | 0.69 (0.41) | 0.49 (0.34) | 0.25 (0.10) |
| SWC (v/v) | 16.21 (5.13) | 19.27 (4.61) | 14.47 (2.91) | 19.23 (1.23) | 10.20 (2.32) |

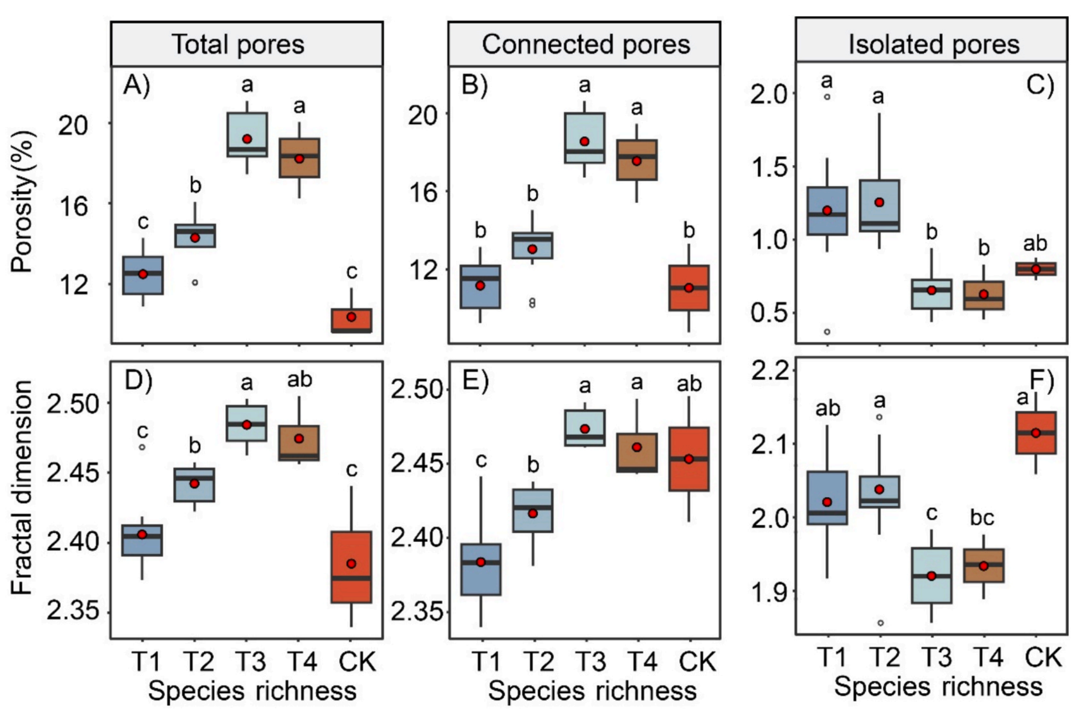


**Fig. 2.** Soil porosity and fractal dimension in different treatments. The boxplots illustrate the variation in (A) total porosity (%), (B) connected porosity (%), (C) isolated porosity (%), (D) fractal dimension of total pores, (E) fractal dimension of connected pores, and (F) fractal dimension of isolated pores across different levels of species richness. The treatments include monocultures (T1), two-species mixtures (T2), three-species mixtures (T3), four-species mixtures (T4), and no planted bare land (CK). Different letters above the boxes denote significant differences among treatments for each parameter ($p < 0.05$). Red dots represent the mean values. For interpretation of the references to color in this figure legend, the reader is referred to the web version of this article.

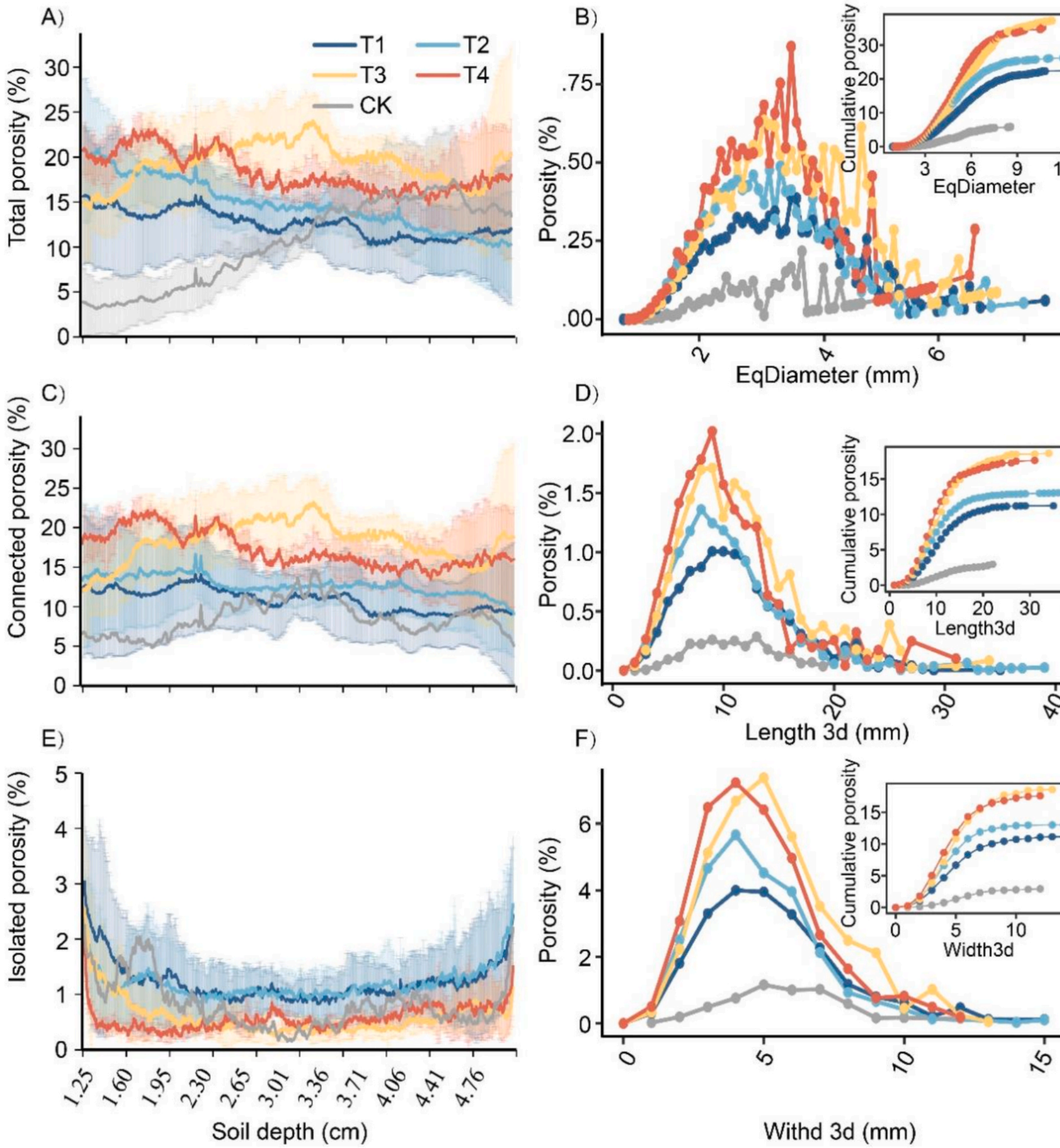


**Fig. 3.** Soil pore characteristics across different plant species richness treatments. Depth profiles of (A) total porosity (B) connected porosity, and (C) isolated porosity, respectively, with solid lines representing treatment means and shaded areas indicating standard error bands. Probability density distributions of (D) equivalent diameter, (E) length, and (F) width of soil pores, with inset cumulative distribution curves. The treatments include monocultures (T1), two-species mixtures (T2), three-species mixtures (T3), four-species mixtures (T4), and no planted bare land (CK).

pores, respectively. The distribution patterns are similar across different treatments, with most connected pores falling within the ranges of 1–5 mm for equivalent diameter, 2–16 mm for length, and 2–8 mm for width. However, within these ranges, treatments with higher species richness exhibit higher porosity values.

Tables 3 and 4 presents the connected pore characteristics for five different treatments. Four species treatment had the highest biopores (0.71 %), however, it is not statistically different from T1-T3. Three species exhibited the highest critical pore dimeters (8.44 mm). Similar, 3 species treatment showed the highest value of EqDiameter, length, Width, Thickness, Area, and volume with 3.84 mm, 11.71 mm, 5.40 mm, 4.62 mm, 892.50 $mm^2$, and 29.30 $mm^3$, respectively. However, these indices showed no significant differences among the five treatments.

### 3.2. Soil saturated and near-saturated hydraulic conductivity in different treatments

Fig. 4 illustrates the effect of species richness on near-saturated and saturated hydraulic conductivity in the soil. The CK treatment exhibited the lowest near-saturated values of 0.067 mm $min^{-1}$ and the lowest saturated hydraulic conductivity values of 0.113 mm $min^{-1}$, respectively. As species richness increased, near-saturated hydraulic conductivity generally increased. The four-species mixture exhibited the highest $K_{nsat}$ value of 0.169 mm $min^{-1}$, marking a statistically significant increase of 125.4 % compared to the unplanted control. Although T4 showed a 74.23 % increase compared to monoculture, this difference was not statistically significant. Similarly, the three-species mixture

**Table 3**
Soil pore characteristics and hydraulic conductivity by species and functional group. Values are means with standard deviations in parentheses. Different lowercase letters indicate significant differences among species within rows (ANOVA, $p < 0.05$).

| Index | *Medicago sativa* (M) | *Astragalus adsurgens* (A) | *Elymus dahuricus* (E) | *Bromus inermis* (B) | Legume | Grass |
|---|---|---|---|---|---|---|
| Porosity (%) | 11.5 (0.34) b | 13.7 (0.33) a | 12.0 (0.75) ab | 12.8 (0.029) ab | 12.58 (1.31) a | 12.39 (0.98) a |
| Fractal dimension (FD, %) | 2.39 (0.01) a | 2.41 (0.00) a | 2.40 (0.01) a | 2.43 (0.02) a | 2.40 (0.01) a | 2.41 (0.03) a |
| Connected porosity (CP, %) | 10.01 (0.62) a | 12.55 (0.54) a | 10.43 (1.80) a | 11.70 (0.31) a | 11.28 (1.48) a | 11.06 (1.35) a |
| CP_FD | 2.35 (0.01) b | 2.39 (0.01) ab | 2.38 (0.02) ab | 2.41 (0.03) a | 2.37 (0.02) a | 2.40 (0.03) a |
| Isolated porosity (IP, %) | 1.46 (0.16) a | 1.13 (0.08) a | 1.10 (0.81) a | 1.10 (0.19) a | 1.30 (0.21) a | 1.10 (0.53) a |
| IP_FD | 2.05 (0.25) a | 2.00 (0.01) a | 2.01 (0.11) a | 2.03 (0.53) a | 2.02 (0.03) a | 2.02 (0.08) a |
| Biopores (%) | 0.35 (0.04) a | 0.31 (0.05) a | 0.38 (0.12) a | 0.41 (0.17) a | 0.36 (0.08) a | 0.36 (0.12) a |
| dc (mm) | 5.34 (0.88) ab | 5.34 (0.88) ab | 5.34 (0.88) ab | 6.62 (1.01) a | 6.23 (3.46) a | 4.44 (2.52) a |
| EqDiameter (mm) | 3.33 (0.06) a | 3.87 (0.20) a | 3.78 (0.61) a | 3.83 (0.17) a | 3.60 (0.32) a | 3.81 (0.41) a |
| Length (mm) | 9.70 (0.67) a | 11.38 (0.79) a | 12.15 (2.67) a | 11.65 (0.63) a | 10.54 (1.13) a | 11.90 (1.75) a |
| Width (mm) | 4.45 (0.31) a | 5.39 (0.42) a | 5.77 (1.80) a | 5.65 (0.76) a | 4.92 (0.61) a | 5.71 (1.24) a |
| Thickness (mm) | 3.84 (0.30) a | 4.57 (0.43) a | 4.96 (1.58) a | 4.95 (0.71) a | 4.21 (0.52) a | 4.96 (1.10) a |
| Area (mm$^2$) | 175.57 (41.94) a | 271.62 (58.06) a | 342.12 (239.04) a | 316.48 (194.61) a | 223.59 (49.42) a | 329.30 (161.53) a |
| Volume (mm$^3$) | 28.77 (2.50) a | 43.58 (5.43) a | 38.81 (17.87) a | 41.02 (7.96) a | 36.17 (8.64) a | 39.92 (12.43) a |
| Shape | 94.61 (55.12) a | 118.00 (53.03) a | 322.50 (349.86) a | 195.36(57.70) a | 106.30 (50.04) a | 258.93 (234.82) a |
| HR | 015 (0.02) a | 015 (0.01) a | 013 (0.02) a | 0.13 (0.01) a | 0.15 (0.13) a | 0.13 (0.02) a |
| Multifractal | 0.07 (0.08) a | 0.33 (0.10) a | 0.28 (0.14) a | 0.14 (0.02) a | 0.20 (0.18) a | 0.21 (0.17) a |
| $K_{sat}$ | 0.17 (0.04) a | 0.14 (0.04) a | 0.17 (0.03) a | 0.16 (0.04) a | 0.15 (0.05) a | 0.16 (0.03) a |
| $K_{nsat}$ | 0.08 (0.03) a | 0.09 (0.04) a | 0.12 (0.05) a | 0.10 (0.03) a | 0.08 (0.02) a | 0.11 (0.04) a |

**Table 4**
Characteristics of the connected pores. The data are presented as mean values with standard deviations in parentheses. Different lowercase letters indicate statistically significant differences among treatments for each parameter ($p < 0.05$). The treatments include monocultures (T1), two-species mixtures (T2), three-species mixtures (T3), four-species mixtures (T4), and no planted bare land (CK).

| Index | T1 | T2 | T3 | T4 | CK |
|---|---|---|---|---|---|
| Biopores (%) | 0.36 (0.029) ab | 0.41 (0.038) ab | 0.41 (0.10) ab | 0.71 (0.27) a | – |
| dc (mm) | 5.34 (0.88) ab | 6.62 (1.01) a | 8.44 (0.75) a | 7.84 (0.97) a | – |
| EqDiameter (mm) | 3.70 (0.34) a | 3.43 (0.22) a | 3.84 (0.24) a | 3.49 (0.20) a | 3.44 |
| Length (mm) | 11.22 (1.58) a | 10.78 (0.98) a | 11.71 (0.95) a | 10.64 (0.1.69) a | 12.29 |
| Width (mm) | 5.31 (1.02) a | 4.81 (0.44) a | 5.40 (0.48) a | 4.87 (0.48) a | 5.98 |
| Thickness (mm) | 4.58 (0.91) a | 4.12 (0.41) a | 4.62 (0.39) a | 4.18 (0.28) a | 5.04 |
| Area (mm$^2$) | 276.45 (130.76) a | 232.02 (64.45) a | 892.5 (70.68) a | 219.69 (47.69) a | 349.39 |
| Volume (mm$^3$) | 23.51 (5.43) a | 24.22 (4.83) a | 29.30 (5.15) a | 23.05 (4.62) a | 19.88 |
| Shape | 182.62 (180.43) a | 140.85 (58.64) a | 157.25 (61.69) a | 115.57 (35.45) a | 575.66 |
| HR | 014 (0.02) a | 0.12 (0.01) a | 0.13 (0.02) a | 0.13 (0.01) a | 0.08 |
| Multifractal | 0.20 (0.05) a | 0.16 (0.44) | 0.20 (0.34) | 0.12 (0.14) a | 0.04 |

Note: CK values represent single observations due to limited connected pore formation in unplanted soil; statistical comparisons were therefore not feasible for this treatment.

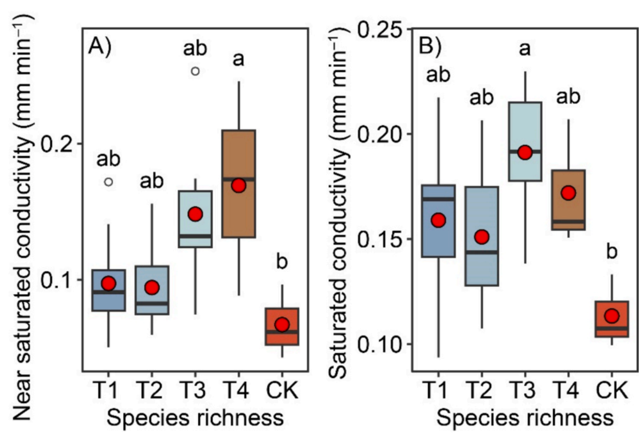


**Fig. 4.** Near-saturated and saturated hydraulic conductivity. The treatments include monocultures (T1), two-species mixtures (T2), three-species mixtures (T3), four-species mixtures (T4), and no planted bare land (CK). Different letters above the boxes denote significant differences among treatments for each parameter ($p < 0.05$). Red dots represent the mean values. (For interpretation of the references to color in this figure legend, the reader is referred to the web version of this article.)

achieved the highest $K_{sat}$ value of 0.172 mm min$^{-1}$, indicating a 129.3 % increase compared to CK, while the 8.18 % increase compared to T1 was not statistically significant.

### 3.3. Soil pores and hydraulic conductivity relationship and species richness effect

Fig. 5 shows the correlation of soil pore parameters and their relationship with both near-saturated and saturated hydraulic conductivity. Near-saturated hydraulic conductivity was significantly positively correlated with porosity, fractal dimension, connected porosity, connected pores fractal dimension and shape factor of biopores, while negatively correlated with isolated porosity and fractal dimension of isolated pores. However, saturated hydraulic conductivity was negatively correlated with EqDiameter, volume, width and hydraulic radius of biopores.

The structural equation model revealed that species richness influenced saturated and near-saturated hydraulic conductivity through distinct pathways (Fig. 6). Species richness directly increased connected porosity led to increased $K_{sat}$. Additionally, the shape factor and volume of biopores indirectly affected $K_{sat}$. For $K_{nsat}$, species richness had a directed positive effect on connected porosity and an indirect positive effect on the shape factor of biopores, ultimately leading to greater near-saturated hydraulic conductivity. Fig. 6 C and D shown the standardized effect size of different factor on $K_{sat}$ and $K_{nsat}$.

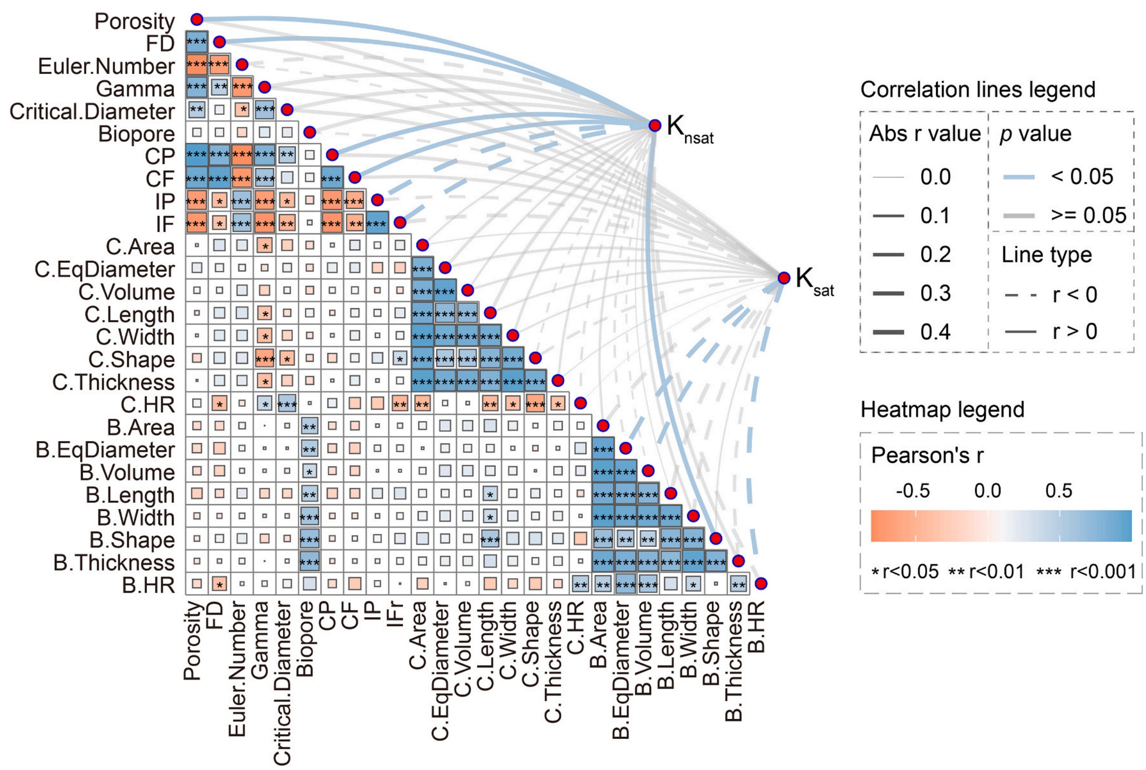


**Fig. 5.** Correlation heatmap and connecting lines between soil pore characteristics and hydraulic conductivity parameters. The heatmap matrix displays Pearson correlation coefficients (r) among all pore characteristics, with color intensity indicating correlation strength (red = negative, blue = positive). Connecting lines link pore characteristics to hydraulic parameters ($K_{sat}$: saturated hydraulic conductivity; $K_{nsat}$: near-saturated hydraulic conductivity). Line thickness represents correlation strength ($|r| = 0.1, 0.2, 0.3, 0.4$), line type indicates correlation direction (solid = $r > 0$, dashed = $r < 0$), and line color denotes statistical significance (blue = $p < 0.05$, gray = $p \geq 0.05$). Variables include: porosity, fractal dimension (FD), Euler number, gamma, critical diameter, biopores, connected porosity (CP), connected porosity fractal dimension (CF), isolated porosity (IP), isolated porosity fractal dimension (IF), and 3D pore descriptors prefixed with C (connected pores) or B (biopores). For interpretation of the references to color in this figure legend, the reader is referred to the web version of this article.

## 4. Discussion

### 4.1. Effect of plant species richness on soil pores characteristics

Our findings indicated that increasing plant diversity led to a significant increase in soil porosity, particularly at plant richness levels of 3 and 4, where total and connected porosity were significantly greater than in monoculture treatments. This result aligns with the findings of Kravchenko et al. (2019) and Wright et al. (2017). Kravchenko et al. (2019) reported that soil pores with diameters between 30–150 μm were more abundant in diverse communities compared to monocultures. Although different pore sizes were detected due to the varying XCT resolution between our study and that of Kravchenko et al. (2019), the results consistently showed higher porosity in diverse plant communities. However, Kravchenko et al. (2021) conducted short-term experiments investigating the effects of different species mixtures on soil pore characteristics, finding that porosity was determined by species identity, rather than diversity level.

The impact of plant diversity on soil porosity can be attributed to three primary, interconnected mechanisms: (1) enhanced soil aggregation, (2) accelerated nutrient cycling, (3) increased biopore formation through root growth (bio-tillage). Firstly, plant diversity promotes soil aggregate stability (Gould et al., 2016). Diverse plant communities, through a wider variety of root architectures and increased root biomass, enhance the production of root exudates (e.g., sugars, organic acids, and amino acids, Eisenhauer et al., 2017; Fujii, 2024). These exudates, along with increased soil fauna activity and improved soil moisture conditions associated with higher plant diversity, stimulate the growth of mycorrhizal fungi (Hallett et al., 2009; Mueller et al., 2024; Wu et al., 2014). Mycorrhizae, in turn, produce glomalin-related soil protein, a "sticky" substance that binds soil particles together (Yang et al., 2024). However, it is important to recognize that microbial activity can have complex, sometimes counteracting effects. For instance, certain microbial communities, fueled by root exudates, can produce hydrophobic compounds that may lead to soil water repellency, potentially impeding infiltration in the uppermost soil layers (Goebel et al., 2011). These processes contribute to the formation and stabilization of soil aggregates (Pohl et al., 2009), leading to a shift in pore size distribution, often characterized by a decrease in micropores and an increase in macropores (Bodner et al., 2014; Lu et al., 2020; Lucas et al., 2022).

Secondly, plant diversity accelerates soil nutrient accumulation, further influencing soil structure and pore characteristics. The presence of multiple plant species with different resource uptake strategies leads to through complementary resource utilization, nutrient enrichment and facilitation among species (Barry et al., 2019; Zhao et al., 2022). As demonstrated in our previous study, plant species richness can alter microbial network characteristics, leading to increased plant-derived carbon and microbial necromass carbon in the short term (Liu et al., 2024). This enhanced nutrient availability, particularly organic matter input, promotes a more favorable soil structure by providing the "glue" that further stabilizes aggregates and influences pore formation (Bucka et al., 2019).

Thirdly, and perhaps most directly, plant diversity influences biopore formation through root growth and activity—a process termed "bio-tillage" (Lucas et al., 2019, 2022). Diverse plant communities exhibit a wider range of root architectures, including variations in root depth, diameter, branching patterns, and lifespan (Ma and Chen, 2016; Oram, 2018). This diversity in root systems leads to the creation of a complex network of biopores as roots penetrate the soil, creating channels as they grow and decompose (Jin et al., 2022). Our findings

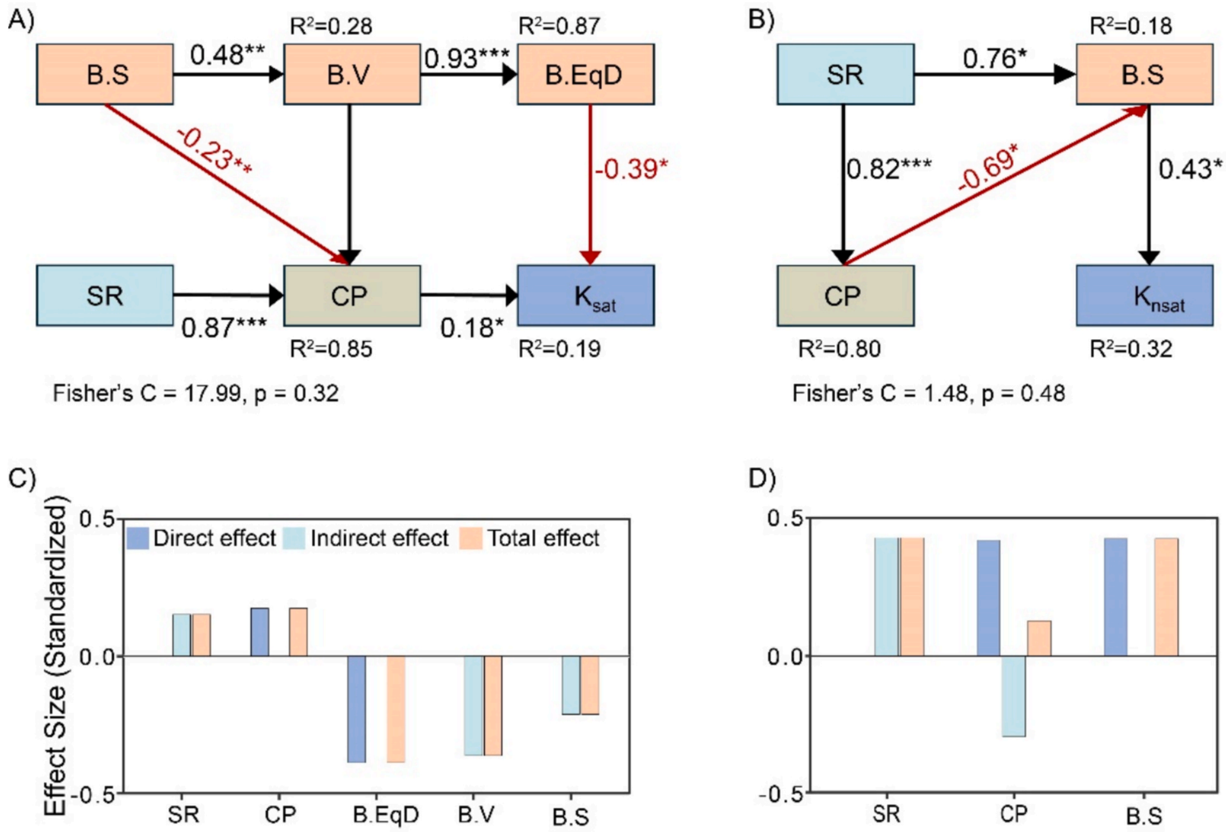


**Fig. 6.** Structural equation model depicting the direct and indirect effects of plant species richness (SR) on saturated hydraulic conductivity ($K_{sat}$) and near-saturated hydraulic conductivity ($K_{nsat}$). SR, Species richness; Connected porosity, CP; Biopore volume, B.V; Biopore equivalent diameter, B.EqD; Biopore shape, B.S. The model illustrates the standardized path coefficients for each significant pathway ($p < 0.05$).

support this, demonstrating that plant species richness increased connected porosity and decreased isolated pores. Moreover, we specifically observed an increase in biopore characteristics with higher species richness, as detailed in our results. These biopores, formed by both living and decaying roots, are crucial for enhancing soil hydraulic conductivity, as they provide preferential pathways for water movement (Gould et al., 2016). The decomposition of roots, which is often faster in diverse communities, leaves behind root channel that contribute to the biopore formation (Oram, 2018). Additionally, higher porosity can facilitate soil nutrient accumulation (Lucas et al., 2023). Furthermore, the continuous wetting and drying cycles near roots, especially pronounced in regions like the Loess Plateau (Ding et al., 2024), contribute to the formation of cracks and fissures that further enhance pore connectivity (Nong et al., 2023; Rasse et al., 2000). These biopores not only facilitate water movement but also improve aeration and provide habitats for soil organisms, further influencing soil structure development (Pires et al., 2017). Although bio-tillage through root growth creates beneficial macropores, soil fauna activity presents contrasting effects. While earthworms create macropore networks, their burrowing can simultaneously compact adjacent soil matrices, reducing porosity in burrow walls through mucus secretion and mechanical compression (Bottinelli et al., 2015; Capowiez et al., 2009). Similarly, while root channels enhance connectivity, excessive fine root density can reduce macroporosity through space occupation and local compaction (Ma et al., 2024a).

### 4.2. *Effect of plant species richness on soil hydraulic conductivity*

Previous studies have reported inconsistent results regarding the effect of plant species richness on soil hydraulic conductivity. While some studies have shown no significant effect or even negative relationships (Blanco-Canqui, 2024), our findings demonstrate that plant species richness significantly increased both saturated and near-saturated hydraulic conductivity. These results align with a growing body of empirical evidence from studies by Wu et al. (2016), Liu et al. (2019) and Ma et al. (2024a), which have also reported positive effects of plant diversity on various measures of soil hydraulic properties.

Wu et al. (2016) found that in artificial grasslands, mixed species plots improved soil infiltration capacity compared to monocultures, primarily due to increased root biomass. Similarly, in a long-term natural restoration grassland, Liu et al. (2019) observed that plant species richness enhanced soil infiltration capacity by increasing soil organic carbon, improving soil aggregate stability and enhancing porosity. Ma et al. (2024a) measured saturated hydraulic conductivity in monoculture and mixed plots of herbs and shrubs and demonstrated that mixed plots exhibited higher hydraulic conductivity. Interestingly, they also found a non-linear relationship between root density and saturated hydraulic conductivity, with an initial decrease and then another decrease as root density increased, suggesting that optimal root density may exist for maximizing hydraulic conductivity.

However, it is important to acknowledge that the relationship between plant diversity and hydraulic conductivity is complex and can be influenced by factors beyond species richness alone. For example, a mechanistic experiment conducted by Gould et al. (2016) in the Jena grassland experiment found that functional group composition, rather than species richness per se, was the primary driver of changes in hydraulic conductivity. They observed that plots dominated by legumes had greater hydraulic conductivity and soil strength compared to those dominated by grasses or forbs, which they attributed to differences in root architecture, such as larger root diameter and greater rooting depth (Gould et al., 2016; Ma et al., 2024a). Our functional group analysis revealed no statistically significant differences between legumes and grasses in monocultures for key hydraulic parameters, suggesting that species-specific traits within functional groups may be more influential than broad functional classifications. This highlights that species identity and functional complementarity, rather than richness alone, determine net hydraulic outcomes (Bardgett et al., 2014). Furthermore, abiotic factors like temperature can also significantly modulate soil hydraulic properties. Our site experiences a wide annual temperature range. Such temperature extremes are known to influence soil water retention, hydraulic conductivity, and gas permeability, particularly in rooted soils, through effects on water viscosity, soil structure (e.g., freeze–thaw cycles), and root growth dynamics (Wang et al., 2023, 2024). While our findings demonstrate a positive effect of herbaceous species richness on $K_{sat}$ under the specific climatic conditions of our study, the magnitude of this effect could potentially be modulated by the prevailing temperature regime.

### 4.3. Mechanisms linking plant species richness, soil pore characteristics and hydraulic conductivity

The observed positive effects of plant species richness on hydraulic conductivity in our study can be explained by the changes in soil pore characteristics driven by increased plant diversity, as discussed in Section 4.1. While soil pores are essential for various soil functions, including water retention and transport, the complex geometry and structure of pores in natural soils make it challenging to establish clear relationships between pore characteristics and hydraulic conductivity. Nevertheless, a systematic review conducted by Basset et al. (2023) revealed that significant correlations between hydraulic conductivity and soil structure are commonly observed, although these relationships can be modified by factors such as soil amendment, crop management and tillage.

Our findings demonstrate that soil hydraulic conductivity was significantly correlated with several pore characteristics, consistent with many previous studies, such as Casali et al. (2024), Ju et al. (2024) and Qian et al. (2024). However, the influence factors of soil pore characteristics on hydraulic conductivity varied across different studies. Porosity, number of macropores, macropores diameter, biopores and connectivity have all been identified as determining factors of hydraulic conductivity. For example, different sizes of soil pores provide varying functions: micropores will regulate carbon sequestration and water retention, while macropores control water transport (Bodner et al., 2023; Li et al., 2024). Additionally, well-connected pores are the primary pathway for water transport, and not all the pores contribute to water movement. Differences in experiment treatment, XCT resolution, and soil texture may be the primary reason for the varying results.

Our findings demonstrate that plant species richness improved hydraulic conductivity by altering pore characteristics, including increased total porosity, connected porosity, biopore formation, and pore fractal dimension. These results are consistent with those of Fischer et al. (2015), who reported that increased porosity and earthworm activity (which can create biopores) were associated with enhanced infiltration capacity in more diverse plant communities. The structural equation modeling results further support the mechanistic link between plant species richness, changing in pore characteristics, and increased saturated and near-saturated hydraulic conductivity.

Consistent with other studies (Casali et al., 2024; Ju et al., 2024; Qian et al., 2024), we found significant correlations between soil hydraulic conductivity and several pore characteristics. However, the specific pore characteristics that most strongly influence hydraulic conductivity can vary across studies, likely due to differences in experimental treatments, soil textures, and the resolution of XCT imaging (Schlüter et al., 2020). For example, while total porosity is often a good predictor, pore connectivity, the presence and characteristics of biopores (e.g., length or tortuosity), and pore size distribution, particularly the proportion of macropores, have also been identified as key factors controlling water movement (Bodner et al., 2023; Fukumasu et al., 2024; Ling et al., 2022).

### 4.4. Implications and limitation

The findings of this study have important implications for sustainable ecosystem management, particularly in addressing environmental challenges such as water scarcity, flooding and climate change (Jung et al., 2021; Leal Filho et al., 2019). By demonstrating that increased plant diversity significantly enhances soil porosity, connectivity, and hydraulic conductivity, this research provides scientific evidence for the role of biodiversity in regulating factors related to the hydrological cycle. These improvements in soil infiltration capacity and water transport under higher plant diversity directly contribute to achieving SDG 6 (Clean Water and Sanitation). Enhanced soil water storage and reduced surface runoff can help ensure the availability and quality of freshwater resources, especially in water-limited regions (Hector, 2022; Keesstra et al., 2012). Furthermore, the positive effects of plant diversity on soil pore structure and hydraulic properties can indirectly support SDG 13 (Climate Action) by enhancing the ability of soil to sequester and store carbon, thereby contributing to climate change mitigation (Kravchenko et al., 2019). Additionally, our findings align with the objectives of SDG 15 (Life on Land) by highlighting the importance of maintaining and restoring terrestrial ecosystems through the conservation of plant biodiversity. The enhanced soil hydrological functions facilitated by diverse plant communities can help sustain the overall health and productivity of land-based ecosystems (Brauman et al., 2007), contributing to their resilience in the face of environmental change (Gao et al., 2023).

However, it is important to acknowledge the limitations of this study and identify areas for future research. The experiment was conducted under controlled field conditions, which may not fully capture the complexity of natural ecosystems, where numerous other biotic and abiotic factors can interact. Additionally, the relatively short-term nature of the study (two growing seasons) means that the long-term effects of plant diversity on soil pore characteristics and hydraulic conductivity remain to be elucidated. Future research should focus on investigating these relationships in more natural field settings over longer time scales (e.g., multiple years to decades), as well as exploring the role of different plant functional groups and their specific traits in driving these processes. Incorporating other factors, such as varying climate conditions, different soil type, and different land management practices, into the experimental design would also provide a more comprehensive understanding of the coupled plant-soil-hydrology system. Furthermore, investigating the potential feedback mechanisms between plant diversity, soil pore structure, and hydrological processes would be valuable for predicting the long-term consequences of biodiversity changes on ecosystem functioning.

## 5. Conclusion

Using X-ray computed tomography for comprehensive soil pore characterization, we quantified the effects of herbaceous species diversity on soil pore structure and hydraulic properties across experimental treatments ranging from monocultures to four-species mixtures. Our results demonstrate that increasing herbaceous plant species richness significantly alters soil pore structure and enhances both saturated and near-saturated hydraulic conductivity through measurable changes in porosity. Specifically, three-species mixtures exhibited the highest total porosity and connected porosity, while simultaneously achieving peak saturated hydraulic conductivity. Conversely, four-species mixtures showed maximal near-saturated hydraulic conductivity. These findings support our hypothesis that increasing herbaceous plant diversity enhances hydraulic conductivity, though the specific physiological and structural mechanisms require further direct investigation. This suggests that managing plant diversity can be a valuable tool for improving soil water storage, reducing surface runoff, and potentially enhancing carbon sequestration.

## CRediT authorship contribution statement

**Huaqing Liu:** Writing – original draft, Investigation, Formal analysis. **Xiaodong Gao:** Writing – review & editing, Supervision, Funding acquisition, Conceptualization. **Long Ma:** Investigation, Formal analysis. **Heng Liu:** Investigation. **Xining Zhao:** Funding acquisition, Conceptualization.

## Declaration of competing interest

The authors declare that they have no known competing financial interests or personal relationships that could have appeared to influence the work reported in this paper.

## Acknowledgements

This research was funded by the National Key Research and Development Program of China (2023YFF1305103, 2021YFD1900700), the National Natural Science Foundation of China (U22A20613), the Cyrus Tang Foundation, the Key Research and Development Program of Shaanxi Province (2023-ZDLNY-49, 2020ZDLNY07-04).

## Data availability

Data will be made available on request.

## References

An, R., Kong, L., Zhang, X., Li, C., 2022. Effects of dry-wet cycles on three-dimensional pore structure and permeability characteristics of granite residual soil using X-ray micro computed tomography. J. Rock Mech. Geotech. Eng. 14, 851–860. https://doi.org/10.1016/j.jrmge.2021.10.004.

Bardgett, R.D., Mommer, L., De Vries, F.T., 2014. Going underground: root traits as drivers of ecosystem processes. Trends Ecol. Evol. 29, 692–699. https://doi.org/10.1016/j.tree.2014.10.006.

Barry, K.E., Mommer, L., van Ruijven, J., Wirth, C., Wright, A.J., Bai, Y., Connolly, J., De Deyn, G.B., de Kroon, H., Isbell, F., Milcu, A., Roscher, C., Scherer-Lorenzen, M., Schmid, B., Weigelt, A., 2019. The future of complementarity: disentangling causes from consequences. Trends Ecol. Evol. 34, 167–180. https://doi.org/10.1016/j.tree.2018.10.013.

Basset, C., Abou Najm, M., Ghezzehei, T., Hao, X., Daccache, A., 2023. How does soil structure affect water infiltration? A meta-data systematic review. Soil Tillage Res. 226, 105577. https://doi.org/10.1016/j.still.2022.105577.

Blanchy, G., Albrecht, L., Bragato, G., Garré, S., Jarvis, N., Koestel, J., 2023. Impacts of soil management and climate on saturated and near-saturated hydraulic conductivity: analyses of the Open Tension-disk Infiltrometer Meta-database (OTIM). Hydrol. Earth Syst. Sci. 27, 2703–2724. https://doi.org/10.5194/hess-27-2703-2023.

Blanco-Canqui, H., 2024. Do cover crop mixtures improve soil physical health more than monocultures? Plant Soil 495, 99–112. https://doi.org/10.1007/s11104-023-06086-4.

Blicharska, M., Smithers, R.J., Mikusiński, G., Rönnbäck, P., Harrison, P.A., Nilsson, M., Sutherland, W.J., 2019. Biodiversity's contributions to sustainable development. Nat. Sustain. 2, 1083–1093. https://doi.org/10.1038/s41893-019-0417-9.

Bodner, G., Leitner, D., Kaul, H.-P., 2014. Coarse and fine root plants affect pore size distributions differently. Plant Soil 380, 133–151. https://doi.org/10.1007/s11104-014-2079-8.

Bodner, G., Zeiser, A., Keiblinger, K., Rosinger, C., Winkler, S.K., Stumpp, C., Weninger, T., 2023. Managing the pore system: Regenerating the functional pore spaces of natural soils by soil-health oriented farming systems. Soil Tillage Res. 234, 105862. https://doi.org/10.1016/j.still.2023.105862.

Bottinelli, N., Jouquet, P., Capowiez, Y., Podwojewski, P., Grimaldi, M., Peng, X., 2015. Why is the influence of soil macrofauna on soil structure only considered by soil ecologists? soil Tillage Res, 146, 118–124. https://doi.org/10.1016/j.still.2014.01.007.

Brauman, K.A., Daily, G.C., Duarte, T.K., Mooney, H.A., 2007. The nature and value of ecosystem services: An overview highlighting hydrologic services. Annu. Rev. Env. Resour. 32, 67–98. https://doi.org/10.1146/annurev.energy.32.031306.102758.

Bucka, F.B., Kölbl, A., Uteau, D., Peth, S., Kögel-Knabner, I., 2019. Organic matter input determines structure development and aggregate formation in artificial soils. Geoderma 354, 113881. https://doi.org/10.1016/j.geoderma.2019.113881.

Capowiez, Y., Cadoux, S., Bouchant, P., Ruy, S., Roger-Estrade, J., Richard, G., Boizard, H., 2009. The effect of tillage type and cropping system on earthworm communities, macroporosity and water infiltration. Soil Tillage Res. 105, 209–216. https://doi.org/10.1016/j.still.2009.09.002.

Casali, E., Larsbo, M., Koestel, J., Jarvis, N., 2024. Macropore flow in relation to the geometry and topology of soil macropore networks: Re-visiting the kinematic wave equation. J. Hydrol. 630, 130732. https://doi.org/10.1016/j.jhydrol.2024.130732.

Chen, K.P., Wei, Y.B., Wu, J.C., 2022. Impact of pore characteristics on displacement processes of air and water flow: modelling and experimental investigation. J. Hydrol. 609, 127691. https://doi.org/10.1016/j.jhydrol.2022.127691.

Cui, Z., Huang, Z., Liu, Y., López-Vicente, M., Wu, G.-L., 2022. Natural compensation mechanism of soil water infiltration through decayed roots in semi-arid vegetation species. Sci. Total Environ. 819, 151985. https://doi.org/10.1016/j.scitotenv.2021.151985.

Ding, Y., Gao, X., Shu, D., Siddique, K.H.M., Song, X., Wu, P., Li, C., Zhao, X., 2024. Enhancing soil health and nutrient cycling through soil amendments: improving the synergy of bacteria and fungi. Sci. Total Environ. 923, 171332. https://doi.org/10.1016/j.scitotenv.2024.171332.

Eisenhauer, N., Lanoue, A., Strecker, T., Scheu, S., Steinauer, K., Thakur, M.P., Mommer, L., 2017. Root biomass and exudates link plant diversity with soil bacterial and fungal biomass. Sci. Rep. 7, 44641. https://doi.org/10.1038/srep44641.

Fang, S., Fell, J., Frank, A., Guo, Y., Herrmann, H.-G., Bähre, D., 2024. Three-dimensional characterization of abrasive chips using micro-computed tomography. Int. J. Adv. Manuf. Technol. 133, 4651–4662. https://doi.org/10.1007/s00170-024-14022-8.

Ferreira, T.R., Archilha, N.L., Cássaro, F.A.M., Pires, L.F., 2023. How can pore characteristics of soil aggregates from contrasting tillage systems affect their intrinsic permeability and hydraulic conductivity? Soil Tillage Res. 230, 105704. https://doi.org/10.1016/j.still.2023.105704.

Ferreira, T.R., Archilha, N.L., Pires, L.F., 2022. An analysis of three XCT-based methods to determine the intrinsic permeability of soil aggregates. J. Hydrol. 612, 128024. https://doi.org/10.1016/j.jhydrol.2022.128024.

Fischer, C., Tischer, J., Roscher, C., Eisenhauer, N., Ravenek, J., Gleixner, G., Attinger, S., Jensen, B., de Kroon, H., Mommer, L., Scheu, S., Hildebrandt, A., 2015. Plant species diversity affects infiltration capacity in an experimental grassland through changes in soil properties. Plant Soil 397, 1–16. https://doi.org/10.1007/s11104-014-2373-5.

Frank, E.H., Charles, D., 2024. Hmisc: harrell miscellaneous.

Fujii, K., 2024. Plant strategy of root system architecture and exudates for acquiring soil nutrients. Ecol. Res. 623–633. https://doi.org/10.1111/1440-1703.12477.

Fukumasu, J., Jarvis, N., Koestel, J., Larsbo, M., 2024. Links between soil pore structure, water flow and solute transport in the topsoil of an arable field: does soil organic carbon matter? Geoderma 449, 117001. https://doi.org/10.1016/j.geoderma.2024.117001.

Gao, X., Wan, H., Zeng, Y., Shao, X., Hu, W., Brocca, L., Yang, M., Wu, P., Zhao, X., 2023. Disentangling the impact of event- and annual-scale precipitation extremes on critical-zone hydrology in semiarid loess vegetated by apple trees. Water Resour. Res. 59, e2022WR033042. https://doi.org/10.1029/2022WR033042.

Goebel, M.O., Bachmann, J., Reichstein, M., Janssens, I.A., Guggenberger, G., 2011. Soil water repellency and its implications for organic matter decomposition - is there a link to extreme climatic events? Glob. Chang. Biol. 17, 2640–2656. https://doi.org/10.1111/j.1365-2486.2011.02414.x.

Gould, I.J., Quinton, J.N., Weigelt, A., De Deyn, G.B., Bardgett, R.D., 2016. Plant diversity and root traits benefit physical properties key to soil function in grasslands. Ecol. Lett. 19, 1140–1149. https://doi.org/10.1111/ele.12652.

Gregory, A.S., Webster, C.P., Watts, C.W., Whalley, W.R., Macleod, C.J.A., Joynes, A., Papadopoulos, A., Haygarth, P.M., Binley, A., Humphreys, M.W., Turner, L.B., Skot, L., Matthews, G.P., 2010. Soil management and grass species effects on the hydraulic properties of shrinking soils. Soil Sci. Soc. Am. J. 74, 753–761. https://doi.org/10.2136/sssaj2009.0284.

Hallett, P.D., Feeney, D.S., Bengough, A.G., Rillig, M.C., Scrimgeour, C.M., Young, I.M., 2009. Disentangling the impact of AM fungi versus roots on soil structure and water transport. Plant Soil 314, 183–196. https://doi.org/10.1007/s11104-008-9717-y.

Haruna, S., Ward, Z., Cartwright, A., Wunner, A., 2023. Influence of no-till cover crops on the physical and hydraulic properties of a Paleudult. Int. Agrophys. 37, 189–199. https://doi.org/10.31545/intagr/162799.

Hector, A., 2022. The importance of biodiverse plant communities for healthy soils. Proc. Natl. Acad. Sci. 119, e2119953118. https://doi.org/10.1073/pnas.2119953118.

Herlinger, R., Vidal, A.C., 2022. X-ray μCt extracted pore attributes to predict and understand Sor using ensemble learning techniques in the Barra Velha Pre-salt carbonates, Santos Basin. Offshore Brazil. J. Petrol. Sci. Eng. 212, 110282. https://doi.org/10.1016/j.petrol.2022.110282.

Hillel, D., 2003. Water Entry into Soil. In: Hillel, D. (Ed.), Introduction to Environmental Soil Physics, 14. Academic Press, Burlington, pp. 259–282. https://doi.org/10.1016/B978-012348655-4/50015-0.

Houston, A.N., Otten, W., Falconer, R., Monga, O., Baveye, P.C., Hapca, S.M., 2017. Quantification of the pore size distribution of soils: assessment of existing software using tomographic and synthetic 3D images. Geoderma 299, 73–82. https://doi.org/10.1016/j.geoderma.2017.03.025.

Isbell, F., Calcagno, V., Hector, A., Connolly, J., Harpole, W.S., Reich, P.B., Scherer-Lorenzen, M., Schmid, B., Tilman, D., van Ruijven, J., Weigelt, A., Wilsey, B.J., Zavaleta, E.S., Loreau, M., 2011. High plant diversity is needed to maintain ecosystem services. Nature 477, 199–202. https://doi.org/10.1038/nature10282.

Jarvis, N., Larsbo, M., Koestel, J., 2017. Connectivity and percolation of structural pore networks in a cultivated silt loam soil quantified by X-ray tomography. Geoderma 287, 71–79. https://doi.org/10.1016/j.geoderma.2016.06.026.

Jin, X., Wang, Z., Wu, F., Li, X., Zhou, X., 2022. Litter mixing alters microbial decomposer community to accelerate tomato root litter decomposition. Microbiol. Spectrum 10, e00186–e00222. https://doi.org/10.1128/spectrum.00186-22.

José, P., Douglas, B., Saikat, D., Deepayan, S., Siem, H., Bert, V.W., Johannes, R., 2024. nlme: linear and nonlinear mixed effects models. Core Team.
Ju, X., Gao, L., She, D., Jia, Y., Pang, Z., Wang, Y., 2024. Impacts of the soil pore structure on infiltration characteristics at the profile scale in the red soil region. Soil Tillage Res. 236, 105922. https://doi.org/10.1016/j.still.2023.105922.
Ju, X., Jia, Y., Li, T., Gao, L., Gan, M., 2021. Morphology and multifractal characteristics of soil pores and their functional implication. Catena 196, 104822. https://doi.org/10.1016/j.catena.2020.104822.
Jung, M., Arnell, A., de Lamo, X., García-Rangel, S., Lewis, M., Mark, J., Merow, C., Miles, L., Ondo, I., Pironon, S., Ravilious, C., Rivers, M., Schepaschenko, D., Tallowin, O., van Soesbergen, A., Govaerts, R., Boyle, B.L., Enquist, B.J., Feng, X., Gallagher, R., Maitner, B., Meiri, S., Mulligan, M., Ofer, G., Roll, U., Hanson, J.O., Jetz, W., Di Marco, M., McGowan, J., Rinnan, D.S., Sachs, J.D., Lesiv, M., Adams, V. M., Andrew, S.C., Burger, J.R., Hannah, L., Marquet, P.A., McCarthy, J.K., Morueta-Holme, N., Newman, E.A., Park, D.S., Roehrdanz, P.R., Svenning, J.-C., Violle, C., Wieringa, J.J., Wynne, G., Fritz, S., Strassburg, B.B.N., Obersteiner, M., Kapos, V., Burgess, N., Schmidt-Traub, G., Visconti, P., 2021. Areas of global importance for conserving terrestrial biodiversity, carbon and water. Nat. Ecol. Evol. 5, 1499–1509. https://doi.org/10.1038/s41559-021-01528-7.
Kassambara, A., 2023. ggpubr: "ggplot2" Based Publication Ready Plots.
Keesstra, S., Geissen, V., Mosse, K., Piiranen, S., Scudiero, E., Leistra, M., van Schaik, L., 2012. Soil as a filter for groundwater quality. Curr. Opin. Env. Sust, 4, 507–516. https://doi.org/10.1016/j.cosust.2012.10.007.
Klöffel, T., Larsbo, M., Jarvis, N., Barron, J., 2024. Freeze-thaw effects on pore space and hydraulic properties of compacted soil and potential consequences with climate change. Soil Tillage Res. 239, 106041. https://doi.org/10.1016/j.still.2024.106041.
Koestel, J., 2018. SoilJ: an ImageJ Plugin for the Semiautomatic Processing of Three-Dimensional X-ray Images of Soils. Vadose Zone J. 17, 1–7. https://doi.org/10.2136/vzj2017.03.0062.
Koestel, J., Dathe, A., Skaggs, T.H., Klakegg, O., Ahmad, M.A., Babko, M., Giménez, D., Farkas, C., Nemes, A., Jarvis, N., 2018. Estimating the permeability of naturally structured soil from percolation theory and pore space characteristics imaged by X-ray. Water Resour. Res. 54, 9255–9263. https://doi.org/10.1029/2018WR023609.
Koestel, J., Schlüter, S., 2019. Quantification of the structure evolution in a garden soil over the course of two years. Geoderma 338, 597–609. https://doi.org/10.1016/j.geoderma.2018.12.030.
Korboulewsky, N., Perez, G., Chauvat, M., 2016. How tree diversity affects soil fauna diversity: a review. Soil Biol. Biochem. 94, 94–106. https://doi.org/10.1016/j.soilbio.2015.11.024.
Kravchenko, A.N., Guber, A.K., Razavi, B.S., Koestel, J., Quigley, M.Y., Robertson, G.P., Kuzyakov, Y., 2019. Microbial spatial footprint as a driver of soil carbon stabilization. Nat. Commun. 10, 3121. https://doi.org/10.1038/s41467-019-11057-4.
Kravchenko, A.N., Zheng, H., Kuzyakov, Y., Robertson, G.P., Guber, A.K., 2021. Belowground interplant carbon transfer promotes soil carbon gains in diverse plant communities. Soil Biol. Biochem. 159, 108297. https://doi.org/10.1016/j.soilbio.2021.108297.
Lange, M., Koller-France, E., Hildebrandt, A., Oelmann, Y., Wilcke, W., Gleixner, G., 2019. How plant diversity impacts the coupled water, nutrient and carbon cycles. In: Mechanisms Underlying the Relationship between Biodiversiy and Ecosystem Function. Elsevier, pp. 185–219.
Larsbo, M., Koestel, J., Jarvis, N., 2014. Relations between macropore network characteristics and the degree of preferential solute transport. Hydrol. Earth Syst. Sci. 18, 5255–5269. https://doi.org/10.5194/hess-18-5255-2014.
Leal Filho, W., Barbir, J., Preziosi, R. (Eds.), 2019. Handbook of climate change and biodiversity, climate change management. Springer International Publishing, Cham.
Lefcheck, J.S., 2016. piecewiseSEM: Piecewise structural equation modelling in r for ecology, evolution, and systematics. Methods Ecol. Evol. 7, 573–579. https://doi.org/10.1111/2041-210X.12512.
Li, Z., Kravchenko, A.N., Cupples, A., Guber, A.K., Kuzyakov, Y., Philip Robertson, G., Blagodatskaya, E., 2024. Composition and metabolism of microbial communities in soil pores. Nat. Commun. 15, 3578. https://doi.org/10.1038/s41467-024-47755-x.
Ling, S., Sun, Y., Sun, D., Jelagin, D., 2022. Pore characteristics and permeability simulation of porous asphalt mixture in pouring semi-flexible pavement. Constr. Build. Mater. 330, 127253. https://doi.org/10.1016/j.conbuildmat.2022.127253.
Liu, H., Gao, X., Li, C., Cai, Y., Song, X., Zhao, X., 2025. Intercropping increases plant water availability and water use efficiency: a synthesis. Agric. Ecosyst. Environ. 109360. https://doi.org/10.1016/j.agee.2024.109360.
Liu, H., Gao, X., Li, C., Ma, L., Siddique, K.H.M., Zhao, X., 2024. Short-term plant mixtures alter soil organic carbon components and microbial network characteristics. Eur. J. Soil Biol. 122, 103650. https://doi.org/10.1016/j.ejsobi.2024.103650.
Liu, Y., Miao, H., Chang, X., Wu, G., 2019. Higher species diversity improves soil water infiltration capacity by increasing soil organic matter content in semiarid grasslands. Land Degrad. Dev. 30, 1599–1606. https://doi.org/10.1002/ldr.3349.
Lu, J., Zhang, Q., Werner, A.D., Li, Y., Jiang, S., Tan, Z., 2020. Root-induced changes of soil hydraulic properties – a review. J. Hydrol. 589, 125203. https://doi.org/10.1016/j.jhydrol.2020.125203.
Lucas, M., Nguyen, L.T.T., Guber, A., Kravchenko, A.N., 2022. Cover crop influence on pore size distribution and biopore dynamics: enumerating root and soil faunal effects. Front. Plant Sci. 13. https://doi.org/10.3389/fpls.2022.928569.
Lucas, M., Santiago, J.P., Chen, J., Guber, A., Kravchenko, A., 2023. The soil pore structure encountered by roots affects plant-derived carbon inputs and fate. New Phytol. 240, 515–528. https://doi.org/10.1111/nph.19159.
Lucas, M., Schlüter, S., Vogel, H.-J., Vetterlein, D., 2019. Soil structure formation along an agricultural chronosequence. Geoderma 350, 61–72. https://doi.org/10.1016/j.geoderma.2019.04.041.
Luo, L., Lin, H., Li, S., 2010. Quantification of 3-D soil macropore networks in different soil types and land uses using computed tomography. J. Hydrol, 393, 53–64. https://doi.org/10.1016/j.jhydrol.2010.03.031.
Luo, Y., Wen, T., Lin, X., Chen, X., Shao, L., 2024. Quantitative analysis of pore-size influence on granite residual soil permeability using CT scanning. J. Hydrol. 645, 132133. https://doi.org/10.1016/j.jhydrol.2024.132133.
Ma, J., Li, Z., Li, P., Ma, B., Xiao, L., Cui, Z., Wang, Z., Min, Z., 2024a. Effect of mixed plant roots on saturated hydraulic conductivity and saturated water content of soil in the loess region. Agric Water Manag 295, 108784. https://doi.org/10.1016/j.agwat.2024.108784.
Ma, J., Ma, B., Li, Z., Wang, C., Shang, Y., Zhang, Z., 2023. Determining the mechanism of the root effect on soil detachment under mixed modes of different plant species using flume simulation. Sci. Total Environ. 858, 159888. https://doi.org/10.1016/j.scitotenv.2022.159888.
Ma, Y., Liu, Y., Rodrigo-Comino, J., López-Vicente, M., Wu, G.-L., 2024b. Mixed-cultivation grasslands enhance runoff generation and reduce soil loss in the restoration of degraded alpine hillsides. Hydrol. Earth Syst. Sci. 28, 3947–3961. https://doi.org/10.5194/hess-28-3947-2024.
Ma, Z., Chen, H.Y.H., 2016. Effects of species diversity on fine root productivity in diverse ecosystems: A global meta-analysis. Glob. Ecol. Biogeogr. 25, 1387–1396. https://doi.org/10.1111/geb.12488.
Mueller, C.W., Baumert, V., Carminati, A., Germon, A., Holz, M., Kögel-Knabner, I., Peth, S., Schlüter, S., Uteau, D., Vetterlein, D., Teixeira, P., Vidal, A., 2024. From rhizosphere to detritusphere – soil structure formation driven by plant roots and the interactions with soil biota. Soil Biol. Biochem. 193, 109396. https://doi.org/10.1016/j.soilbio.2024.109396.
Müller, K., Katuwal, S., Young, I., McLeod, M., Moldrup, P., de Jonge, L.W., Clothier, B., 2018. Characterising and linking X-ray CT derived macroporosity parameters to infiltration in soils with contrasting structures. Geoderma 313, 82–91. https://doi.org/10.1016/j.geoderma.2017.10.020.
Naveed, M., Moldrup, P., Schaap, M.G., Tuller, M., Kulkarni, R., Vogel, H.-J., Wollesen de Jonge, L., 2016. Prediction of biopore- and matrix-dominated flow from X-ray CT-derived macropore network characteristics. Hydrol. Earth Syst. Sci. 20, 4017–4030. https://doi.org/10.5194/hess-20-4017-2016.
Nespoulous, J., Merino-Martín, L., Monnier, Y., Bouchet, D.C., Ramel, M., Dombey, R., Viennois, G., Mao, Z., Zhang, J.-L., Cao, K.-F., Le Bissonnais, Y., Sidle, R.C., Stokes, A., 2019. Tropical forest structure and understorey determine subsurface flow through biopores formed by plant roots. Catena 181, 104061. https://doi.org/10.1016/j.catena.2019.05.007.
Ni, J.J., Leung, A.K., Ng, C.W.W., 2018. Modelling soil suction changes due to mixed species planting. Ecol. Eng. 117, 1–17. https://doi.org/10.1016/j.ecoleng.2018.02.023.
Nong, R., Wan, Y., Ding, Y., Chai, M., Zhu, L., 2023. Effects of root systems on crack formation: experiments, modeling, and analyses. Soil Tillage Res. 233, 105784. https://doi.org/10.1016/j.still.2023.105784.
Oram, N.J., 2018. Root interactions in a diverse grassland : the role of root traits in belowground productivity and decomposition (Doctoral dissertation). Wageningen University, Wageningen.
Pires, L.F., Borges, J.A.R., Rosa, J.A., Cooper, M., Heck, R.J., Passoni, S., Roque, W.L., 2017. Soil structure changes induced by tillage systems. Soil Tillage Res. 165, 66–79. https://doi.org/10.1016/j.still.2016.07.010.
Pohl, M., Alig, D., Körner, C., Rixen, C., 2009. Higher plant diversity enhances soil stability in disturbed alpine ecosystems. Plant Soil 324, 91–102. https://doi.org/10.1007/s11104-009-9906-3.
Qian, Y., Yang, X., Zhang, Z., Li, X., Zheng, J., Peng, X., 2024. Estimating the permeability of soils under different tillage practices and cropping systems: Roles of the three percolating pore radii derived from X-ray CT. Soil Tillage Res. 235, 105903. https://doi.org/10.1016/j.still.2023.105903.
Quigley, K.M., Kolka, R., Sturtevant, B.R., Dickinson, M.B., Kern, C.C., Miesel, J.R., 2021. Restoring open canopy pine barrens from the ground up: Repeated burns correspond with increased soil hydraulic conductivity. Sci. Total Environ. 767, 144258. https://doi.org/10.1016/j.scitotenv.2020.144258.
Rabot, E., Wiesmeier, M., Schlüter, S., Vogel, H.-J., 2018. Soil structure as an indicator of soil functions: a review. Geoderma 314, 122–137. https://doi.org/10.1016/j.geoderma.2017.11.009.
R Development Core Team., 2023. R: a language and environment for statistical computing. R Foundation for Statistical Computing, Vienna. http://www.R-project.org. Accessed 30 Dec 2024.
Ramos, T.B., Gonçalves, M.C., Martins, J.C., van Genuchten, M.T., Pires, F.P., 2006. Estimation of soil hydraulic properties from numerical inversion of tension disk infiltrometer data. Vadose Zone J. 5, 684–696. https://doi.org/10.2136/vzj2005.0076.
Rasse, D.P., Smucker, A.J.M., Santos, D., 2000. Alfalfa root and shoot mulching effects on soil hydraulic properties and aggregation. Soil Sci. Soc. Am. J. 64, 725–731. https://doi.org/10.2136/sssaj2000.642725x.
Rieu, M., Sposito, G., 1991. Fractal fragmentation, soil porosity, and soil water properties: I. Theory. Soil Sci. Soc. Am. J. 55, 1231–1238. https://doi.org/10.2136/sssaj1991.03615995005500050006x.
Rujner, H., Leonhardt, G., Marsalek, J., Viklander, M., 2018. High-resolution modelling of the grass swale response to runoff inflows with mike SHE. J. Hydrol. 562, 411–422. https://doi.org/10.1016/j.jhydrol.2018.05.024.

Schlüter, S., Sammartino, S., Koestel, J., 2020. Exploring the relationship between soil structure and soil functions via pore-scale imaging. Geoderma 370, 114370. https://doi.org/10.1016/j.geoderma.2020.114370.

Shao, X., Gao, X., Zhang, Z., He, N., Ma, N., Du, X., Zhao, X., 2024. Deep (200–2,000 cm) soil water use can compensate for the drought effect on gas exchange in dry years better than in wet years for dryland tree plantations. Water Resour. Res. 60, e2024WR037084. https://doi.org/10.1029/2024WR037084.

Stolze, K., Barnes, A.D., Eisenhauer, N., Totsche, K.U., 2022. Depth-differentiated, multivariate control of biopore number under different land-use practices. Geoderma 418, 115852. https://doi.org/10.1016/j.geoderma.2022.115852.

Talukder, R., Plaza-Bonilla, D., Cantero-Martínez, C., Wendroth, O., Lampurlanés, J., 2023. Soil hydraulic properties and pore dynamics under different tillage and irrigated crop sequences. Geoderma 430, 116293. https://doi.org/10.1016/j.geoderma.2022.116293.

Tang, Y., Pan, H., Zhang, T., Cao, L., Wang, Y., 2024. The dynamics of soil macropores and hydraulic conductivity as influenced by the fibrous and tap root systems. Agriculture 14, 1676. https://doi.org/10.3390/agriculture14101676.

Tilman, D., 2000. Causes, consequences and ethics of biodiversity. Nature 405, 208–211. https://doi.org/10.1038/35012217.

Vervoort, R.W., Cattle, S.R., 2003. Linking hydraulic conductivity and tortuosity parameters to pore space geometry and pore-size distribution. J. Hydrol, 272, 36–49. https://doi.org/10.1016/S0022-1694(02)00253-6.

Wang, H., Chen, R., Leung, A.K., Garg, A., Jiang, Z., 2025. Pore-based modeling of hydraulic conductivity function of unsaturated rooted soils. Int. J. Numer. Anal. Meth. Geomech. 49, 1790–1803. https://doi.org/10.1002/nag.3958.

Wang, H., Chen, R., Leung, A.K., Gui, L., Wu, F., 2024. Modelling nonisothermal gas conductivity function of unsaturated rooted soils. Int. J. Heat Mass Transf. 229, 125744. https://doi.org/10.1016/j.ijheatmasstransfer.2024.125744.

Wang, H., Chen, R., Leung, A.K., Huang, J., 2023. Temperature effects on the hydraulic properties of unsaturated rooted soils. Can. Geotech. J. 60. https://doi.org/10.1139/cgj-2022-0475.

Wang, M., Xu, S., Kong, C., Zhao, Y., Shi, X., Guo, N., 2019. Assessing the effects of land use change from rice to vegetable on soil structural quality using X-ray CT. Soil Tillage Res. 195, 104343. https://doi.org/10.1016/j.still.2019.104343.

Wang, N., Zhang, T., 2024. Soil pore structure and its research methods: A review. Soil Water Res. 19, 1–24. https://doi.org/10.17221/64/2023-SWR.

Wang, W., Wang, Y., Sun, Q., Zhang, M., Qiang, Y., Liu, M., 2018. Spatial variation of saturated hydraulic conductivity of a loess slope in the south jingyang plateau, china. Eng. Geol. Special Issue: Loess Engineering Properties and Loess Geohazards 236, 70–78. https://doi.org/10.1016/j.enggeo.2017.08.002.

Webb, B., Robinson, D.A., Marshall, M.R., Ford, H., Pagella, T., Healey, J.R., Smith, A.R., 2022. Variation in root morphology amongst tree species influences soil hydraulic conductivity and macroporosity. Geoderma 425, 116057. https://doi.org/10.1016/j.geoderma.2022.116057.

Wickham, H., Chang, W., Henry, L., Pedersen, T.L., Takahashi, K., Wilke, C., Woo, K., Yutani, H., Dunnington, D., Brand, T. van den, Posit, PBC, 2024. ggplot2: Create elegant data visualisations using the grammar of graphics. https://CRAN.R-project.org/package=ggplot2.

Wright, A.J., de Kroon, H., Visser, E.J.W., Buchmann, T., Ebeling, A., Eisenhauer, N., Fischer, C., Hildebrandt, A., Ravenek, J., Roscher, C., Weigelt, A., Weisser, W., Voesenek, L.A.C.J., Mommer, L., 2017. Plants are less negatively affected by flooding when growing in species-rich plant communities. New Phytol. 213, 645–656. https://doi.org/10.1111/nph.14185.

Wu, G., Liu, Y., Yang, Z., Cui, Z., Deng, L., Chang, X., Shi, Z., 2017. Root channels to indicate the increase in soil matrix water infiltration capacity of arid reclaimed mine soils. J. Hydrol. 546, 133–139. https://doi.org/10.1016/j.jhydrol.2016.12.047.

Wu, G., Yang, Z., Cui, Z., Liu, Y., Fang, N., Shi, Z., 2016. Mixed artificial grasslands with more roots improved mine soil infiltration capacity. J. Hydrol. 535, 54–60. https://doi.org/10.1016/j.jhydrol.2016.01.059.

Wu, Q., Cao, M., Zou, Y., He, X., 2014. Direct and indirect effects of glomalin, mycorrhizal hyphae and roots on aggregate stability in rhizosphere of trifoliate orange. Sci. Rep. 4, 5823. https://doi.org/10.1038/srep05823.

Yang, H., Wang, G., Wang, J., Xiao, Q., Li, Z., De Clerck, C., Meersmans, J., Colinet, G., Zhang, W., 2024. No-tillage facilitates soil organic carbon sequestration by enhancing arbuscular mycorrhizal fungi-related soil proteins accumulation and aggregation. Catena 245, 108323. https://doi.org/10.1016/j.catena.2024.108323.

Yang, H., Xu, H., Zhang, W., Li, Z., Fan, H., Lambers, H., Li, L., 2022. Overyielding is accounted for partly by plasticity and dissimilarity of crop root traits in maize/legume intercropping systems. Funct. Ecol. 36, 2163–2175. https://doi.org/10.1111/1365-2435.14115.

Yu, F., Sun, D., Hu, M., Wang, J., 2019. Study on the pores characteristics and permeability simulation of pervious concrete based on 2D/3D CT images. Constr. Build. Mater. 200, 687–702. https://doi.org/10.1016/j.conbuildmat.2018.12.135.

Zhang, F., Li, S., Yue, S., Song, Q., 2022a. The effect of long-term soil surface mulching on SOC fractions and the carbon management index in a semiarid agroecosystem. Soil Tillage Res. 216, 105233. https://doi.org/10.1016/j.still.2021.105233.

Zhang, H., He, H., Gao, Y., Mady, A., Filipović, V., Dyck, M., Lv, J., Liu, Y., 2023. Applications of Computed Tomography (CT) in environmental soil and plant sciences. Soil Tillage Res. 226, 105574. https://doi.org/10.1016/j.still.2022.105574.

Zhang, R., 1997. Determination of soil sorptivity and hydraulic conductivity from the disk infiltrometer. Soil Sci. Soc. Am. J. 61, 1024–1030. https://doi.org/10.2136/sssaj1997.03615995006100040005x.

Zhang, W., Surigaoge, S., Yang, H., Yu, R.-P., Wu, J.-P., Xing, Y., Chen, Y., Li, L., 2024. Diversified cropping systems with complementary root growth strategies improve crop adaptation to and remediation of hostile soils. Plant Soil. https://doi.org/10.1007/s11104-023-06464-y.

Zhang, Y., Peng, S., Chen, X., Chen, H.Y.H., 2022b. Plant diversity increases the abundance and diversity of soil fauna: a *meta*-analysis. Geoderma 411, 115694. https://doi.org/10.1016/j.geoderma.2022.115694.

Zhang, Z., Liu, K., Zhou, H., Lin, H., Li, D., Peng, X., 2019. Linking saturated hydraulic conductivity and air permeability to the characteristics of biopores derived from X-ray computed tomography. J. Hydrol. 571, 1–10. https://doi.org/10.1016/j.jhydrol.2019.01.041.

Zhao, L., Gao, X., He, N., Zhao, X., 2022. Ecohydrological advantage of young apple tree-based agroforestry and its response to extreme droughts on the semiarid Loess Plateau. Agric. For. Meteorol. 321, 108969. https://doi.org/10.1016/j.agrformet.2022.108969.

Zhao, X., Wu, P., Gao, X., Tian, L., Li, H., 2014. Changes of soil hydraulic properties under early-stage natural vegetation recovering on the loess plateau of China. Catena 113, 386–391. https://doi.org/10.1016/j.catena.2013.08.023.

Zheng, H., Guber, A.K., Kuzyakov, Y., Zhang, W., Kravchenko, A.N., 2022. Plant species and plant neighbor identity affect associations between plant assimilated C inputs and soil pores. Geoderma 407, 115565. https://doi.org/10.1016/j.geoderma.2021.115565.